Applied Mathematics, Modeling and Computer Simulation
C.-H. Chen et al. (Eds.)

doi:10.3233/ATDE221096

Investigation of the Displacement Transfer Characteristic and Parameter Optimization Design of Fluid-Elastic Isolator

Zhenkun LI [a,b, 1], Qiyou CHENG [a,b], Qian FENG[a,b], Chen LIU [a,b], Yan ZHU [a,b], Fengnan SUN [a,b]

[a] *Science and Technology on Rotorcraft Aeromechanics Laboratory, Jingdezhen 333001, China*

[b] *China Helicopter Research and Development Institute, Jingdezhen 333001, China*

Abstract. The main parameters influencing the displacement transfer rate of the fluid-elastic isolator are studied and optimized. Firstly, the equation of motion is derived by applying the Lagrange principle. The effects of the main design parameters on the displacement transfer rate of the fluid-elastic isolator are analyzed. Secondly, parameter optimization design is conducted by employing the genetic algorithm for a civil helicopter. by Aiming at the minimum displacement transfer rate, the optimal parameters are determined. Lastly, the criterion for parameter optimization design is proposed considering both the displacement transfer rate and the weight cost. Design parameters with a high vibration isolation rate and low weight are obtained. Results reveal that the vibration isolation behavior of a fluid-elastic vibration isolator depends on the coupling effects of multiple parameters. The parameters obtained by the genetic algorithm demonstrate a higher vibration isolation rate than the ordinary parameter design. Based on the optimization criterion, the fluid elastic isolator possesses a higher vibration isolation rate and lower weight cost than the experimental result in the literature. And it will be helpful for the parameter design of the fluid elastic isolator.

Keywords. Fluid-elastic Vibration Isolator, Displacement Transfer rate, Parameter Optimization Design, Genetic Algorithm, Parameter Optimization Design Criterion

1. Introduction

The fluid-elastic isolator is an effective helicopter vibration reduction method, and researchers have conducted massive research on it [1-5].

Eurocopter carried out research on the active control of the fluid-elastic vibration isolator based on the passive fluid-elastic vibration isolator [6]. The LORD Corporation developed a variety of fluid-elastic vibration isolators with different vibration reduction frequencies, and experimental research was carried out on different types of helicopters [4] to verify the vibration reduction effect of the fluid-elastic vibration isolator. Han et al. [7] designed a fluid-elastic vibration isolator model that can be used for the main rotor

1 Corresponding Author, Zhenkun LI, No. 6, Hangkong Road, Zhushan District, Jingdezhen City, Province Jiangxi; E-mail: 550880903@qq.com.

with variable pitch rods. Qian Feng et al. [8] tested the dynamic stiffness and static stiffness of the designed fluid-elastic vibration isolator, and the theoretical results were consistent with the experimental values. Deng [9] conducted sensitivity analysis on the material parameters and structural parameters of the fluid-elastic vibration isolator, and the influence of the design parameters on the dynamic characteristics of the vibration isolator was studied.

It is seen that parameter analysis and experimental verification on the fluid-elastic vibration isolator have been carried out. However the parameter optimization design method has not been formed, and parameter optimization design criteria has not been established yet. In this paper, the dynamic model of the fluid-elastic vibration isolator is constructed. And based on the genetic algorithm, the main parameters affecting the transmission efficiency of the fluid-elastic vibration isolator are optimized. The experimental results in the literature are compared to verify the effectiveness of the optimization algorithm and the optimization design criteria.

2. Theoretical Modelling of the Fluid-elastic Isolator

The theoretical model of the fluid-elastic isolator is shown in figure 1. The inertial liquid exists in the upper and lower liquid chambers and the inertial channel.

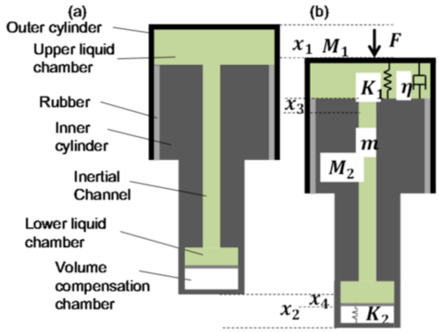

Figure 1. Mechanical model of the system

The material properties and displacements of each component are shown in figure 1. The cross-section area of the upper liquid chamber, the lower liquid chamber and are denoted as Au, Ad, and A0 respectively. The amplification ratios are defined as R1=Au/A0, R2=Ad/A0. The mass M_1 at the upper end of the vibration isolator is subjected to an external harmonic excitation $F=f\cos(\omega t)$. The total kinetic energy, potential energy, and dissipative energy are respectively.

$$\begin{aligned} T &= \frac{1}{2}M_1\dot{x}_1^2 + \frac{1}{2}M_2\dot{x}_2^2 + \frac{1}{2}m\left(\dot{x}_2 + \dot{x}_3\right)^2, \\ V &= \frac{1}{2}K_1\left(1+i\eta\right)\left(x_1 - x_2\right)^2 + \frac{1}{2}K_2x_4^2, \\ Q &= \frac{1}{2}c\dot{x}_3^2 \end{aligned} \tag{1}$$

Then the governing equations can be derived from the generalized Lagrange principle.

$$\frac{d}{dt}\left(\frac{\partial L}{\partial \dot{q}_j}\right)-\frac{\partial L}{\partial q_j}+\frac{\partial Q}{\partial \dot{q}_j}=F_j \tag{2}$$

where L=T-V; q_j (j=1, 2) is generalized coordinate; F_j is the external force on an object. According to the law of the conservation of mass, there is the following relationship between the liquid passing through the inertia channel section and the displacement of the upper and lower liquid chambers.

$$A_u\left(x_1-x_2\right)=A_0x_3=A_dx_4, x_3/\left(x_1-x_2\right)=R_1, x_3/x_4=R_2, \tag{3}$$

Substituting Eq. (3) into Eq. (1) and eliminating x_3 and x_4, substituting the resultant equations into Eq. (2), the governing equations of the system can be obtained.

$$\mathrm{M}\,\ddot{\mathrm{X}}+\mathrm{C}\,\dot{\mathrm{X}}+\mathrm{K}\,\mathrm{X}=\mathrm{F} \tag{4}$$

where,

$$\begin{aligned}
&\mathrm{M}=\begin{bmatrix} M_1+mR_1^2 & mR_1\left(1-R_1\right) \\ mR_1\left(1-R_1\right) & M_2+m\left(1-R_1\right)^2 \end{bmatrix}, \mathrm{C}=\begin{bmatrix} cR_1^2 & -cR_1^2 \\ -cR_1^2 & cR_1^2 \end{bmatrix}, \\
&\mathrm{K}=\frac{1}{R_2^2}\begin{bmatrix} K_1R_2^2+K_2R_1^2 & -K_1R_2^2-K_2R_1^2 \\ -K_1R_2^2-K_2R_1^2 & K_1R_2^2+K_2R_1^2 \end{bmatrix}, \mathrm{X}=\begin{bmatrix} x_1 \\ x_2 \end{bmatrix}, \mathrm{F}=\begin{bmatrix} f\cos\left(\omega t\right) \\ 0 \end{bmatrix}
\end{aligned} \tag{5}$$

Setting the ratio of the displacement at the lower end of the isolator to the displacement at the upper end of the isolator as the displacement transfer rate, x_2/x_1, the displacement transfer rate T_d can be obtained.

$$T_d=\frac{x_2}{x_1}=\frac{K_1R_2^2+K_2R_1^2-m\omega^2R_2^2R_1\left(R_1-1\right)+i\left(c\omega R_1^2R_2^2+\eta R_2^2\right)}{K_1R_2^2+K_2R_1^2-M_2\omega^2R_2^2-m\omega^2R_2^2\left(R_1-1\right)^2+i\left(c\omega R_1^2R_2^2+\eta R_2^2\right)} \tag{6}$$

By neglecting the dampings (ie c=0, η=0), the ideal vibration isolation frequency (i.e. anti-resonance frequency) and resonant frequency can be obtained from Eq. (6).

$$\begin{aligned}
&\omega_1=\frac{1}{2\pi}\sqrt{\frac{K_1R_2^2+K_2R_1^2}{mR_2^2R_1\left(R_1-1\right)}}, \\
&\omega_2=\frac{1}{2\pi}\sqrt{\frac{K_1R_2^2+K_2R_1^2}{R_2^2\left[M_2+m\left(R_1-1\right)^2\right]}}
\end{aligned} \tag{7}$$

3. Analysis of Transfer Characteristics of The Fluid-Elastic Isolator

The rotor vibration load transmitted by the hub is the main vibration source of the helicopter, and its main frequency component is $N\Omega$, where N and Ω are the number of blades and the rotor speed respectively. Thus, there is ω=$N\Omega$ in Eq. (5). Further, it can be obtained from Eq. (6) that T_d is related to the rubber stiffness K_1, the lower liquid chamber stiffness K_2, the liquid mass m of the inertia channel, the amplification ratios R_1 of the upper liquid chambers, the amplification ratios R_2 of the lower liquid chambers, the rubber loss factor η, and the liquid viscous damping c [7, 10]. Decomposing m, R_1, and R_2, the displacement transfer rate is also related to the inertial channel length l, radius r, liquid density ρ, the upper liquid chamber radius R_u and the lower liquid chamber radius R_d.

It is noted that some of the above parameters are not independent, they are coupled with each other. For example, changing the radius of the inertial channel will affect the liquid mass m and the amplification ratios R_1 and R_2 in the inertial channel at the same time. Taking K_1, K_2, r, l, R_u, and R_d as the research objects, the influence of the six main design parameters on the transfer characteristics of the vibration isolator is analyzed.

The influences of the stiffness K_1 and K_2 on the displacement transfer rate are shown in figure 2, in which the value of the excitation frequency on the abscissa has been normalized by the rotor speed NΩ. The change of stiffness K_1 and K_2 will affect the optimal vibration isolation frequency. At the anti-resonance frequency point (with the lowest displacement transfer rate), when K_1 is increased, the displacement transfer rate of the anti-resonance frequency point increases. However, when K_2 increases, the displacement transfer rate of the anti-resonance frequency point decreases.

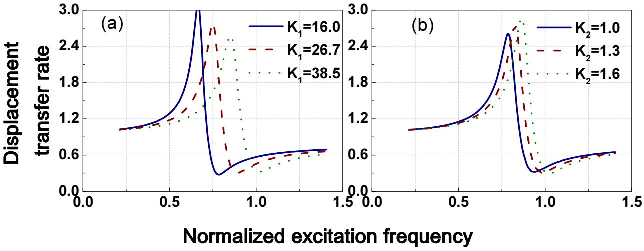

(a) T_d with different K_1 (b) T_d with different K_2

Figure 2. Displacement transfer rate with different K_1 and K_2

Figure 3 summarizes the change of the transfer characteristics with the upper liquid chambers radius R_u and the lower liquid chambers radius R_d. R_u and R_d can adjust the anti-resonance frequency point greatly. R_u and R_d are negatively correlated with the optimal vibration isolation frequency: as R_u and R_d increase, the amplification ratio increases, and the optimal vibration isolation frequency decreases.

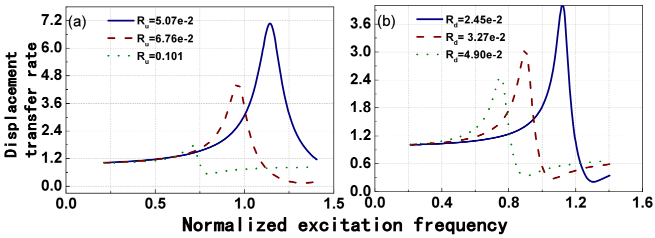

(a) T_d with different R_u (b) T_d with different R_d

Figure 3. Displacement transfer rate with different R_u and R_d

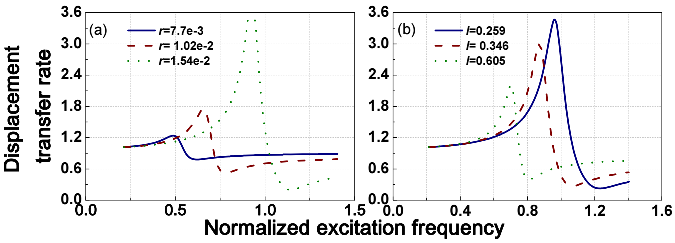

(a) T_d with different r (b) T_d with different l

Figure 4. Displacement transfer rate with different r and l

The change of the transfer characteristics with the inertial channel radius r and length l is shown in figure 4. The magnitude of r affects the amplification ratios R_1, R_2 and the inertial liquid mass m at the same time. When r increases, the optimal vibration isolation frequency increases, and the displacement transfer rate decreases. When l increases, the optimal vibration isolation frequency decreases, and the optimal displacement transfer rate decreases. It can be seen from figure 6 that an appropriate increase in the liquid mass of the inertial channel can obtain better transfer characteristics, but it is necessary to pay attention to the extra mass and weight cost.

4. Parameters Optimization Design

Based on the previous section, it can be seen that a single parameter will affect multiple variables of the transfer characteristics. Therefore it is difficult to determine the required design parameters one by one from the analysis of a single parameter. Thus the genetic algorithm is applied to optimize the design of the main parameters of the fluid-elastic vibration isolator.

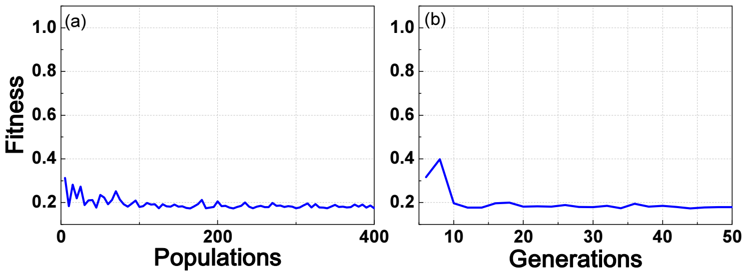

(a) Fitness with different populations (b) Fitness with different generations

Figure 5. The fitness with different populations and generations

According to the value range of the material property (such as K_1) and the structural size range, parameter optimization design is carried out, and the displacement transfer rate is set as the fitness index. The parameter value range is shown in table 1. All parameters in table 1 have been normalized by constants of the same dimension unit of a helicopter. For example, the length of the inertial channel l is normalized by the length of the main gearbox. Naming the optimization condition at this time as condition 1, and taking the displacement transfer rate as the fitness function,

$$\min\left[f(x)\right]=\min\left[\frac{K_1R_2^2+K_2R_1^2-m\omega^2R_2^2R_1\left(R_1-1\right)+i\left(c\omega R_1^2R_2^2+\eta R_2^2\right)}{K_1R_2^2+K_2R_1^2-M_2\omega^2R_2^2-m\omega^2R_2^2\left(R_1-1\right)^2+i\left(c\omega R_1^2R_2^2+\eta R_2^2\right)}\right] \tag{8}$$

Figure 5 shows the relationship between the optimal fitness and the initial population size and the number of generations. To meet the convergence requirements, the parameter optimization design of this study takes 400 populations and 50 iterations.

Table 1. Range of the dimensionless design parameters

Parameters	Range	Parameters	Range
K_1	[29.2, 48.8]	R_d	[1.36 e-2, 0.272]
K_2	[0.98, 9.76]	l	[0.27, 0.69]
R_u	[1.36 e-2, 0.272]	r	[6.8,27.2]e-3

Under the above settings, the obtained design parameters and optimal fitness (minimum displacement transfer rate) are shown in Condition 1 in table 2. The displacement transfer rate is 17%, which is much lower than the results of the fluid-elastic vibration isolator given in the literature [8, 11], which proves the effectiveness of the genetic algorithm for optimizing the transfer characteristics.

Table 2. Fitness and parameters in different Conds. (conditions)

Conds.	K_1	K_2	R_u	R_d	l	r	T_d	m_{fe}	F_n
1	29.28	0.98	0.0729	0.0728	0.6185	0.0161	17.1%	0.516	**0.346**
2	35.14	1.0	0.0823	0.0819	0.6812	0.0196	20.5%	0.700	**0.454**
3	35.14	1.0	0.0553	0.0304	0.6812	7.9e-3	27.1%	0.156	**0.214**
Ref.[11]	35.14	1.0	0.0840	0.0408	0.504	9.8e-3	30%	0.221	**0.261**

It is noted that the material properties K_1 and K_2 in engineering material cannot be valued continuously as in table 1. In most cases, they can only be selected from several specific values for different types of materials. Material properties K_1 and K_2 in reference [11] are chosen, the remaining four structural parameters are optimized, and the optimization condition is named condition 2.

The design parameters and optimal fitness (minimum displacement transfer rate) obtained at this time are shown in Condition 2-table 1. The displacement transfer rate of the fluid-elastic vibration isolator is 20%, only 67% of in the literature [11] (displacement transfer rate of 30%). From the perspective of displacement transfer rate, the genetic algorithm can achieve a better optimization effect.

Comparing condition 2 with the result in the literature [11], more weight is needed, which might be unacceptable for helicopters that are sensitive to total empty weight. Therefore, both the displacement transfer rate and weight cost should be considered in the parameter optimization design. And the parameter optimization design criteria suitable for the fluid-elastic vibration isolator is then proposed.

$$F_n = W_t T_d + \left(1 - W_t\right) m_{fe} \tag{9}$$

where m_{fe} is the dimensionless mass of the fluid-elastic vibration isolator, obtained by the ratio of the mass of a single fluid-elastic vibration isolator to 1% of the mass of the whole helicopter. W_t is the weighting coefficient of the displacement transfer rate T_d, $0< W_t <1$. F_n is the weighted fitness coefficient, the smaller the F_n, the better the parameter optimization design effect.

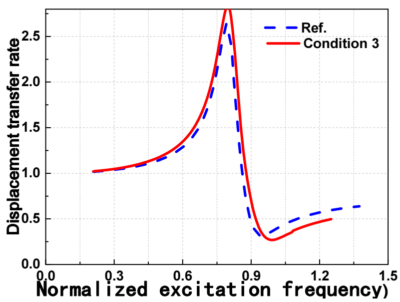

Figure 6. Comparison of condition 3 and Ref. [11]

Based on condition 2, the mass m_{fe} is calculated, and the weighting coefficient is taken as W_t =0.5, and the optimization condition is recorded as condition 3.

The optimal parameters and optimal fitness under condition 3 are shown in condition 3-table 2. The weighted fitness coefficients F_n are listed in the last column of table 2, with F_{n3} =0.214 for condition 3 and F_{nr} =0.261 for the reference [11]. It is seen that the optimization effect in condition 3 is better than in the literature since $F_{n3} < F_{nr}$.

As shown in figure 6, the displacement transfer rate of condition 3 is 27.4% while 30% for the literature at NΩ (i.e. $\omega/N\Omega=1$). The optimized displacement transfer rate is slightly lower than the result in the literature, indicating a better vibration reduction effect. The dimensionless mass of condition 3 is 0.156, and with 0.221 in the literature, indicating the isolator is 30% lighter than in the literature. The displacement transfer rate is lower, and the weight of the vibration isolator is smaller under condition 3, which proves the validity of the proposed parameter design criteria.

Comparing the four conditions in table 2, conditions 1 and 2 pay more weight to achieve a lower displacement transfer rate. The total mass of the fluid-elastic vibration isolator under condition 1 is 2-3 times that of condition 3 and the literature. Taking condition 2 as an example, the mass of a single vibration isolator reaches 0.7% of the weight of the helicopter, and the weight of the entire vibration isolation system (with 4 isolators) will far exceed 1% of the weight of the whole helicopter, which is unacceptable. Therefore, the weighted fitness coefficient F_n is a more suitable parameter design criterion. It can be seen from table 2 that $Fn_3<F_{nr}<F_{n1}<F_{n2}$, that is, the parameter optimization of condition 3 is the most reasonable.

5. Conclusions

Theoretical modeling is conducted based on the two-dimensional fluid-elastic model, and 6 main parameters that affect the displacement transfer rate are analyzed. The genetic algorithm is employed to optimize the parameters. A parameter optimization design criteria is proposed considering the displacement transfer rate and the mass cost.

Parametric analysis reveals that the main parameters would change the anti-resonance point. The optimal displacement transfer rate is negatively related to R_u、R_d、l. A single parameter would cause a complex influence on the transfer rate, therefore the overall effects of different parameters should be taken into consideration when conducting parameter optimization.

Employing the genetic algorithm, the resultant displacement transfer rate is far lower than the results in the literature. Based on the material property in the literature, four structural parameters are optimized, and the obtained displacement transfer rate is still lower. Based on the proposed parameter optimization design criteria F_n, the parameters in the literature are optimized. Compared with the results in the literature, the obtained fluid-elastic vibration isolator has a lower displacement transfer rate and also lower weight cost. Therefore the validity of the proposed parameter optimization criteria is verified.

Acknowledgement

This work was financially supported by foundation of national key laboratory KT-JJ-THKZ-WDZC.

References

[1] Kyle R. Vibration Analysis and Testing of Bell 429 Helicopter[C]. American Helicopter Society 66th Annual Forum.Phoenix Arizona, May, 2010

[2] Han Dong, Rahn Christopher D and SMITH Edward C, Higher harmonic pitch link loads reduction using fluidlatic isolators [J]. Journal of Aerospace Engineering, 228(3) 455–469, 2014

[3] Mcgurie Dennis P. Active Vibration Control Using Fluidlastic Pylon Struts[C]. American Helicopter Society 62nd Annual Forum, Phoenix, Arizona May 9-11, 2006

[4] Halwes D R. LIVE – Liquid Inertia Vibration Eliminator[C]. American Helicopter Society 36th Annual Forum.Washington, D.C., May 1980

[5] Cheng Qiyou, Deng Jinghui, Qian Feng et al. Dynamic Performance Analysis and Design for a Fluidlastic Isolator[C]. ICRCA, July 26–28, 2019, Guangzhou, China

[6] Konstanzer Peter. Recent advances in Eurocopter's passive and active vibration control[C]. American Helicopter Society 64th Annual Forum, 2008

[7] Dong Han, Christopher D Rahn, Edward C Smith. Higher harmonic pitch link loads reduction using fluidlastic isolators, Journal of Aerospace Engineering, 228(3): 455-469, 2014

[8] Qian Feng, Cheng Qiyou, Dai Zhixiong. Design and Test Analysis of Fluidlastic Isolator [J]. Equipment Environmental Engineering, 09:52-57, 2020

[9] Cheng Qiyou, Deng Jinghui, Feng Zhizhuang, et al. Analysis of material parameter effects on fluidlastic isolators performance [C]//NMCI, November 18-20, 2017, Sanya, China

[10] Rodrigues Jonathan, Cranga Paul, CHESNE Simon et al. Hybrid active suspension system of a helicopter main gearbox [J]. Journal of Vibration and Control, 24(5):956-974, 2016

[11] Deng Jinghui. Theoretical Modeling and Experimental Study of Fluid-elastic Isolator [J]. Journal of Northwestern Polytechnical University, 40(1), 182-188, 2022